ICSE6-204

An Air-Bubble Screen Used as a Countermeasure to Reduce Erosion in Open-Channel bends

Violaine DUGUÉ[1], Koen BLANCKAERT[1,2] and Anton J. SCHLEISS[1]

[1]Laboratory of Hydraulic Constructions (LCH),
Ecole Polytechnique Fédérale de Lausanne (EPFL), Station 18, CH-1015 Lausanne, Switzerland.
e-mail : violaine.dugue@epfl.ch, koen.blanckaert@epfl.ch, anton.schleiss@epfl.ch

[2]State key at Laboratory of Urban and Regional Ecology, Research Center for Eco-Environmental Sciences,
Chinese Academy of Sciences, Beijing.

In open-channel bends, interactions between streamwise flow, curvature-induced secondary flow and sediment transport lead to a typical bar-pool bed topography. Erosion occurs near the outer bank that can endanger structures, whereas deposition occurs near the inner bank that can reduce the navigable width.
Laboratory experiments have been performed in a sharp open-channel bend to investigate how a bubble screen can influence the bend hydrodynamics and morphological evolution. A porous tube placed near the outer bank and connected at both ends to a pressurized-air system generated a bubble screen strong enough to counteract the descending velocities of the curvature-induced secondary flow.
Foregoing clear-water scour experiments with and without the bubble screen have shown that the bubble screen modifies the velocity distribution and acts directly on the bend morphology by shifting the region of maximum scour further away from the outer bank.
In the reported study, similar experiments have been performed under live-bed conditions. Measurements of the three-dimensional flow field and topography were compared and allowed estimating the beneficial effect of the bubble screen. In the upstream part of the bend, the redistribution of velocity pattern is not sufficient to strongly modify the morphology whereas at the downstream part of the bend, the scour hole is reduced and shifted from the outer bank to the middle of the cross-section.

Key words

Open-channel bend, Morphodynamics, Erosion, Bubble screen

I INTRODUCTION

Open-channel bend flows are characterized by complex interactions between the streamwise flow, the curvature-induced secondary flow and the bed morphology [Odgaard, 1981; Struiksma, 1985; Whiting, 1993; Blanckaert, 2001]. These interactions lead to the development of a typical bar-pool bed topography with a main scour hole near the outer bank which can endanger foundations and a point bar at the inner bend which might reduce the navigable width of the river.

The two major controlling measures employed for preventing the development of the scour hole and the point bar, reported in literature, are (i) the protection of the bed with a permanent construction such as a fixed outer bend layer [Roca, 2007, 2009], or (ii) influencing the flow patterns, for example with the addition of bottom vanes [Odgaard, 1983].

A new way of influencing the flow has been investigated at LCH-EPFL in a sharply curved laboratory channel. A bubble screen placed near the outer bank can generate upward velocities and surface currents, which result in the generation of a bubble-induced secondary flow. Under its influence, the mean velocity as well as the bed shear stress patterns are redistributed around the bend [Blanckaert, 2008]. If the bubble screen is properly located, the curvature-induced secondary flow can be counteracted and shifted towards the inner bank. Figure 1 schematically illustrates the working principle of this new technique.

Bubble screens, plumes or curtains have already been used in hydraulic field to contain density intrusion [Nakai, 2002] or for lake destratification [Schladow, 1993]. They may represent an ecological and non-

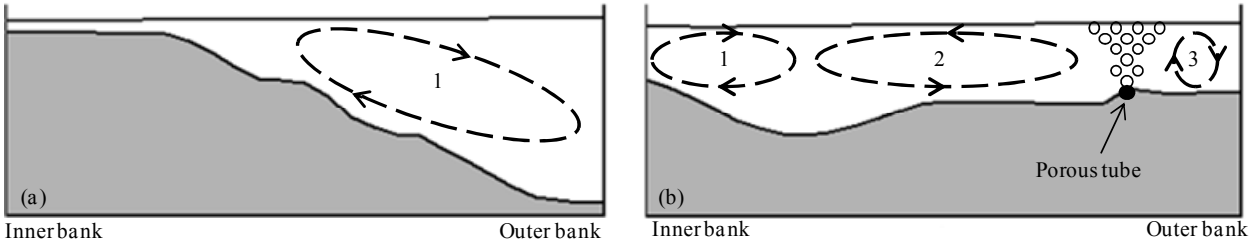

Figure 1: Conceptual sketches of the bubble screen working principle.

(Left) Reference configuration without the bubble screen. (Right) Bubble screen configuration. Schematic indication of secondary flows: curvature-induced secondary flow (1), inner bubble-induced secondary flow (2), and outer bubble-induced secondary flow (3).

permanent alternative to avoid fixed constructions in rivers.

Previous experiments performed under clear-water scour conditions have revealed that the bend morphology can be dramatically modified by the action of the bubble screen. Scour was shifted near the inner bank and the point bar no longer developed [Dugué, 2011].

In the continuity of previous investigations, two experiments with and without the bubble screen have been performed under live-bed conditions and similar hydraulic conditions until the morphological equilibrium was obtained. Patterns of streamwise flow, curvature-induced and bubble-induced secondary flows, and final bed morphology have been investigated.

The objective of the present paper is to gain insight in the morphodynamic mechanisms induced by the bubble screen under live-bed conditions. Morphologic and hydrodynamic comparisons of the two experiments are provided in the present paper and aim at answering the following questions:

- What is the impact of a bubble screen on the general bend morphology under live-bed conditions?
- How is the mean velocity pattern influenced by the use of the bubble screen?

The paper presents briefly the experimental set-up and procedure, then provides morphological comparisons of the two experiments with and without bubble screen and finally discusses the hydrodynamic changes induced by the bubble screen in two representative cross-sections in the bend.

II EXPERIMENTAL SET-UP AND PROCEDURE

II.1 Experimental set-up

Experiments were performed in a sharply curved open-channel bend of constant width B = 1.3 m that consists of a 9 m long upstream straight reach, followed by a 193° bend with a constant centreline radius of curvature R = 1.7 m, and finished by a 5 m long downstream straight reach (Figure 2a). The banks are vertical and made of smooth Plexiglas.

A curvilinear reference system (s, n, z) was adopted where s represents the streamwise direction, the transverse n axis points in the outward direction and the vertical z axis in the upward direction.

The flume bed was filled with a quasi-uniform quartz sand with a mean diameter of 2 mm. During experiments, sediment was continuously fed into the flume near the entrance at a constant rate (q_s = 0.025 kg/(m.s)) by means of a back-and-forth moving scraper. At the end of the flume, a settling tank was installed to allow the deposition of the transported sediment.

The bubble screen was generated by means of a porous tube placed on the bottom of the channel, ballasted with a chain to avoid large amplitude movements and connected to its both ends to the laboratory air-pressure device. The porous tube started 0.1 m before the entry of the bend to allow the establishment of the bubble screen before the entry of the bend and finished at the end of the flume after the downstream straight part. The porous tube was located at 0.2 m from the outer bank. The air pressure was controlled by means of a manometer and the air discharge measured by means of a rotameter.

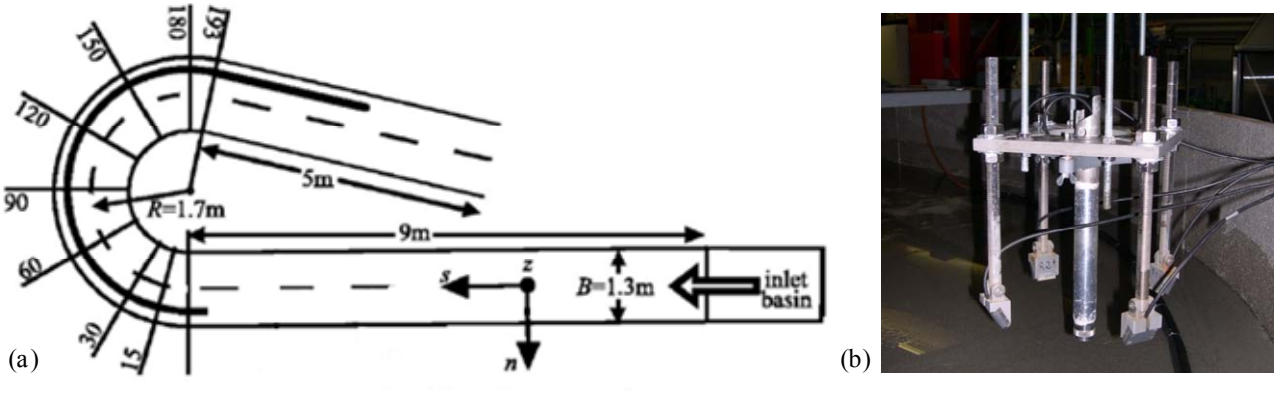

Figure 2: (a) Experimental set-up and (b) Acoustic Doppler Velocity Profiler (ADVP).

II.2 Instrumental devices

Velocity patterns were measured in the cross-sections at 15, 30, 60, 90, 120, 150 and 180° in the bend by means of an Acoustic Doppler Velocity Profiler (ADVP), developed at EPFL. The ADVP consists of a central emitter surrounded by four receivers (Figure 2b) and measures the quasi-instantaneous velocity vector along an entire profile. From these measurements, the time-averaged velocities in the three directions (v_s, v_n and v_z) are derived. More information on the ADVP process and accuracy estimations have been reported by Lemmin [1997], Hurther [1998] and Blanckaert [2006]. Data treatment procedures of ADVP measurements and near-surface extrapolations are described in detail in Blanckaert [2010].

Vertical profiles were measured in each cross-section every 0.05 m in the range n = -0.45 m to n = 0.45 m in the reference experiment without the bubble screen and in the range n = -0.45 m to n = 0.35 m when using the bubble screen. Velocity measurements were not possible near the bubble screen because the bubbles interfered with the acoustic signal of the ADVP.

ADVP measurements were performed under live-bed conditions, involving migrating bedforms. Bed elevation in the measured cross-section was documented before and after the ADVP measurements to estimate the bed level variation during the entire cross-section measurement.

At the end of the experiment, water surface elevation was documented by means of a point gauge. The final bed elevation was measured on a refined grid using a laser distometer (every 5 cm in the transversal axis on the range n = -0.6 m to n = 0.6 m, and every 5° in the streamwise axis of the bend).

II.3 Experimental conditions

Two experiments were performed under live-bed conditions with a constant sediment feeding. Main experimental conditions of both experiments are summarized in Table 1.

One reference experiment without the bubble screen, M75_14_00, and one experiment with the bubble screen, MB75_14_p6_d20, were conducted on an initially horizontal bed until an equilibrium morphology with superimposed migrating bedforms was obtained.

Label	Q *(l/s)*	q_s *(kg/(m.s))*	Pa *(kPa)*	H *(m)*	U *(m/s)*	E_s *(10^{-4})*	R/B *(-)*	R/H *(-)*	B/H *(-)*
M75_14_00	75	0.025	-	0.14	0.41	-28.40	1.31	12.1	9.2
MB75_14_p6_d20	75	0.025	600	0.14	0.41	-28.40	1.31	12.1	9.2

Table 1: Experimental conditions.

Q is the water discharge, q_s is the sediment discharge, *Pa* is the chosen air-pressure, *H* is the final flume-averaged flow depth, *U* is the flume-averaged velocity, E_s is the flume-averaged energy slope. Experiments are labelled by the experiment configuration (M=mobile bed, MB= mobile bed with bubble screen), the discharge [l/s], the water depth [cm], the air pressure [bar] and the distance between the porous tube and the outer bank [cm].

III RESULTS AND DISCUSSION

III.1 Influence of the bubble screen on the bend morphology

Figure 3 illustrates in detail the final bed elevation for the two experiments. The bed reference level for each experiment (z = 0 m) coincides with the flume-averaged bed level.

In the upstream part of the bend, both experiments are characterized by morphological features typical for sharply curved bends [Roca, 2007; Abad, 2009; Blanckaert, 2010]. A main scour hole develops between the cross-sections at 40° and 100°. According to literature, this scour hole is induced by the impingement of the upstream straight flow on the outer bank and by the abrupt reversal of flow near the bed [Ferguson, 2003; Blanckaert, 2010]. At the same time, a point bar develops at the inner bend.

However, downstream of the cross-section at 100° in the bend, morphological features diverge between the two experiments. In the reference experiment, the point bar extends until 2 m in the downstream straight part whereas with the use of the bubble screen, the point bar stops at the cross-section at 150° in the bend. Between the cross-sections at 100° and 150° in the reference experiment, the transverse bed slope is reduced and four mesoscopic bedforms occurred with a maximal amplitude occurring near the outer bank.

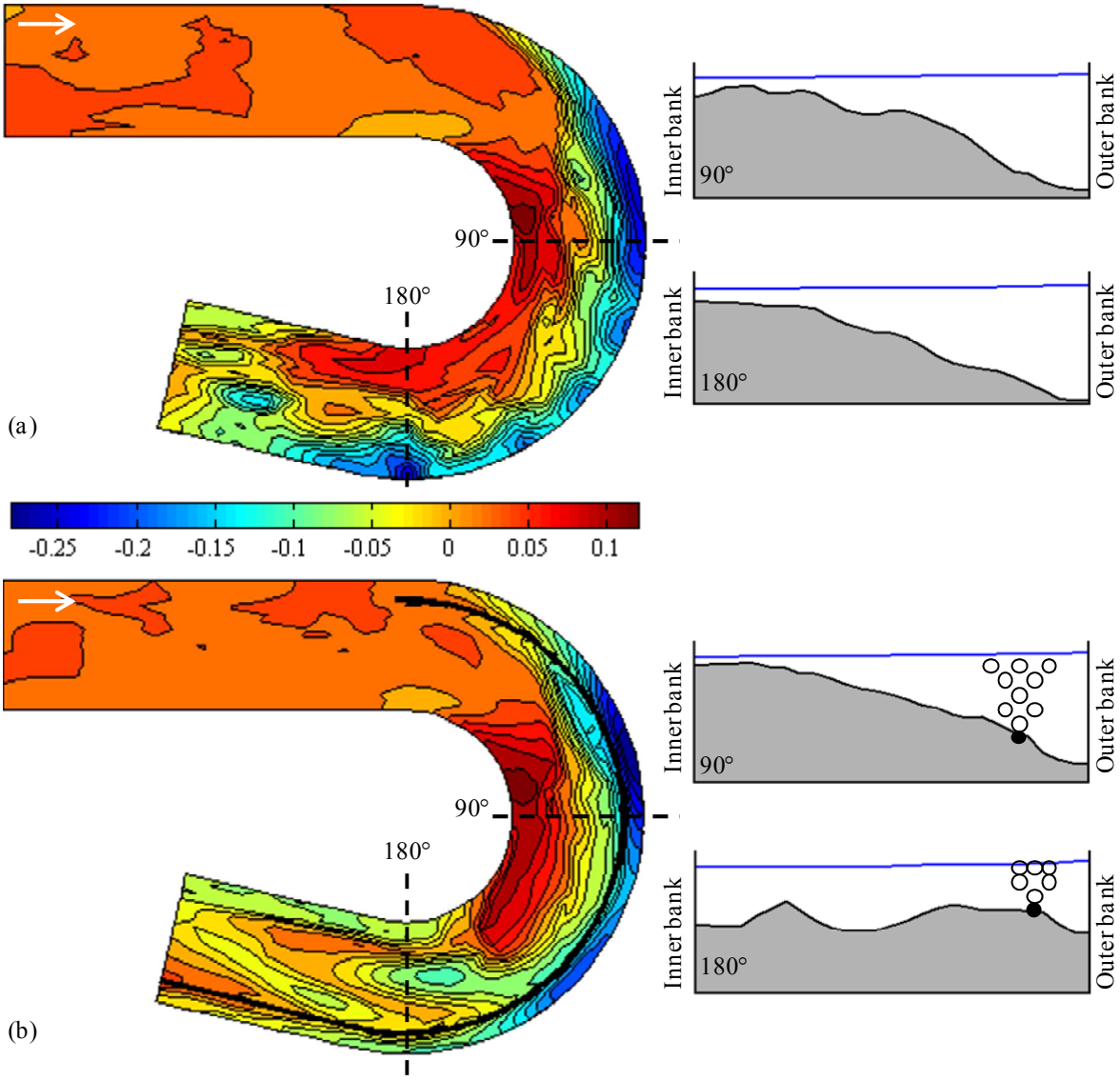

Figure 3: Morphological comparison of M75_14_00 and MB75_14_p6_d20 experiments.

(Left) Isolines of the final bed level with an interval of 0.02 m derived from laser altimetry measurements for the M75_14_00 (a) and MB75_14_p6_d20 (b) experiments. The same color scale has been used to simplify comparison. (Right) Water surface and bed elevation in the cross-section at 90° and 180° in the bend for the M75_14_00 (top) and MB75_14_p6_d20 (bottom) experiments.

With the bubble screen, the mesoscopic bedforms do not appear near the outer bank but a shallow hole with the same depth than the amplitude of the previous dunes (z = -0.17 cm) is observed.

In the downstream part of the bend, between cross-sections at 170° and 193°, a second scour hole can be observed in the reference experiment. According to Frothingam [2003] and Blanckaert [2010], this scour hole is promoted by the still dominant curvature-induced secondary flow, which advects the core of maximum streamwise velocities near the base of the outer bank. This second scour hole is considerably reduced and is shifted from near the outer bank to the middle part of the cross-section when using the bubble screen. The point bar migration seems to be blocked by the development of the second scour hole in the middle of the cross-section at 175° in the bend.

The morphological modification induced by the bubble screen can be further observed in the cross-sections at 90° and 180° in the bend where the two main scour holes are located in the reference experiment (Figure 3 right). In the cross-section at 90°, the bed profile is found to be similar in both experiments. However, in the cross-section at 180°, the transverse bed slope has been considerably reduced and the scour hole has been shifted from near the outer bank to the middle of the cross-section and its depth has been reduced from z = -0.22 m to z = -0.08 m.

III.2 Influence of the bubble screen on the velocity redistribution

In order to explain the different morphological impact of the bubble screen between cross-sections at 90° and 180° in the bend, the present section will compare the flow field measured in these two cross-sections with and without the bubble screen.

Figures 4 and 5 illustrate the bed topography, the water surface elevation and the three components (streamwise, transverse and vertical) of the velocity vector in the cross-section at 90° and at 180° in the bend, respectively.

In the cross-section at 90° in the bend (Figure 4), the bottom shape is similar with and without the use of the bubble screen. In the reference experiment without bubble screen, the core of maximum streamwise velocity is located between n = 0.2 m and n = 0.4 m and maximal velocity are of 0.65 m/s. The curvature-induced secondary flow typical of open-channel bends can be observed in the transverse and vertical velocity

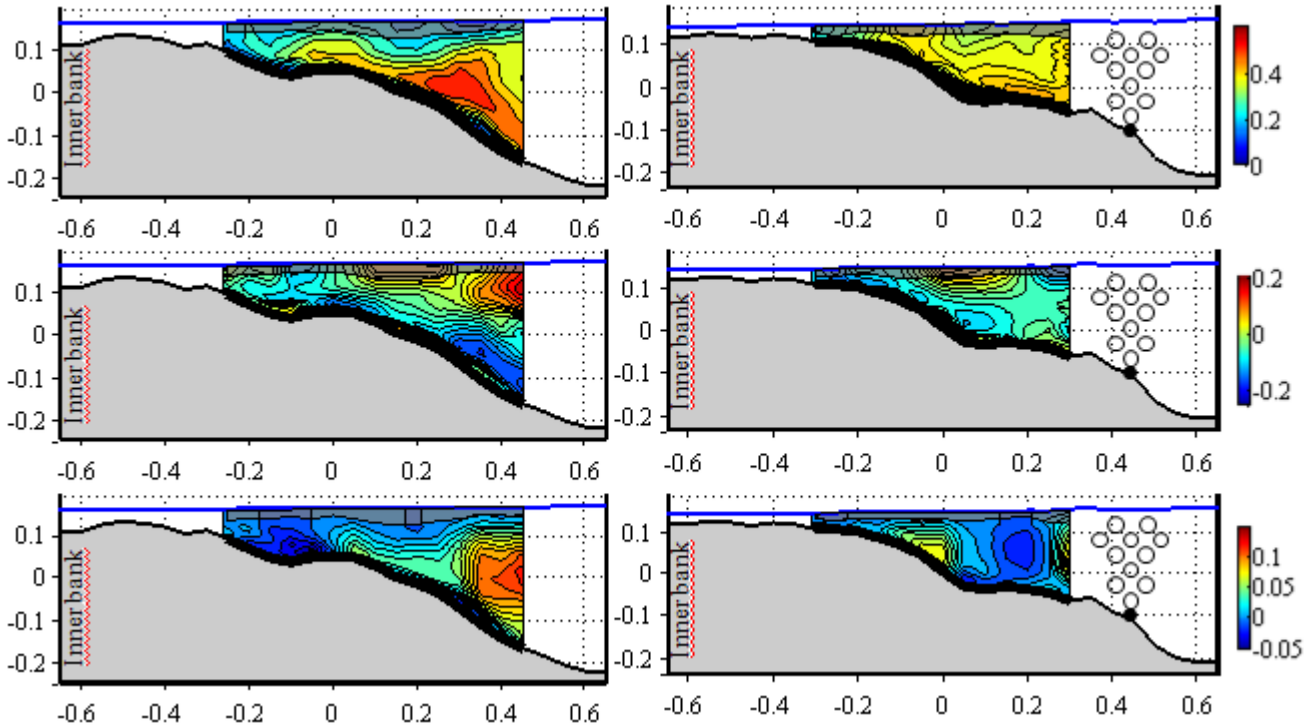

Figure 4: Hydrodynamic comparison of M75_14_00 and MB75_14_p6_d20 experiments in the cross-section at 90° in the bend.

Measured patterns of the (top) streamwise, (middle) transverse, and (bottom) vertical velocities in the cross-section at 90° in the M75_14_00 (left) and the MB75_14_p6_d20 (right) experiments. The dashed area near the water surface indicates the area bridged by means of extrapolations.

distributions. Outward transverse flow extends near the surface in the outer half of the cross-section and negative transverse velocities occurs near the bed. The core of upward velocity is located near the outer bank at n = 0.45 m, indicating that downward velocities occurs very near the outer bank. In the presence of the bubble screen, a negative transverse current can be observed with a transverse extent from about n = 0.3 m to about n = 0.2 m. The curvature-induced secondary flow still exists but extends from n = -0.1 m to n = 0.2 m. Its strength has been considerably reduced. The core of maximum streamwise velocity does not occur at the same location than in the reference experiment and should be located very near the outer bank. Finally, downward velocities are observed at n = 0.2 m, where the curvature-induced and the bubble-induced secondary flows meet.

The mean velocity patterns have been strongly modified in this cross-section by the use of the bubble screen. However, the transversal bed shapes are similar in both experiments and should be related to maximum streamwise velocities located very near the outer bank. In this cross-section, the bubble screen seems to be too weak to counteract the flow impingement and the scour depth is similar in this first scour hole with and without the use of the bubble screen.

In the downstream part of the bend (Figure 5), the velocity patterns and the morphology have been dramatically modified by the presence of the bubble screen. In the reference experiment, a pronounced transverse slope can be observed with a maximal scouring depth of -0.22 m near the outer bank. A secondary flow is observed with strong outwards velocities near the water surface and inwards velocities near the bend such as in the cross-section at 90° in the bend (Figure 4). Downward velocities can be observed at n = 0.2 m but the core of maximal downward velocities is supposed to be located very near from the outer bank as well as maximum streamwise velocities.

With the use of the bubble screen, the bed elevation is almost flat with one scour hole (z = -0.05 m) near the outer bank which is probably related to the existence of the outer bubble-induced secondary flow (Figure 1) and one scour hole (z = -0.08 m) located in the middle of the cross-section and related to the inner bubble-induced secondary flow. Strong inwards velocity are observed near the water surface and extend from n =-0.1 m to the position of the porous tube (n = 0.45 m). Several secondary flow cells can be observed in this cross-section: a first one located very near the bubble screen and two in the middle of the cross-section probably related to the point bar which is located just upstream. Moreover, the streamwise velocity location is extended to the outer half cross-section reducing the high-streamwise velocity concentration near the outer bank and consequently reducing erosion near the outer bank.

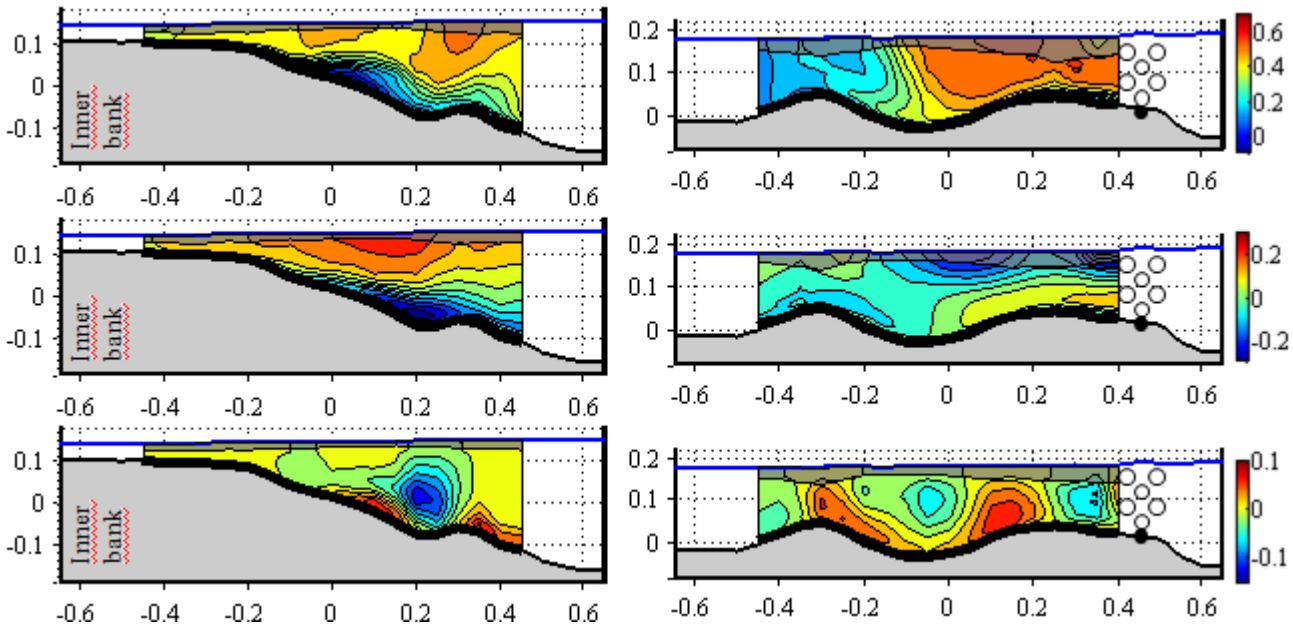

Figure 5: Hydrodynamic comparison of M75_14_00 and MB75_14_p6_d20 experiments in the cross-section at 180° in the bend.

Measured patterns of the (top) streamwise, (middle) transverse, and (bottom) vertical velocities in the cross-section at 180° in the M75_14_00 (left) and the MB75_14_p6_d20 (right) experiments. The dashed area near the water surface indicates the area bridged by means of extrapolations.

Finally, the bubble screen is found to be more efficient in the downstream straight part of the bend and is able to modify the velocity patterns as well as the bed morphology.

IV CONCLUSIONS

These experiments show that an air-bubble screen can be used for influencing bend morphodynamics. In the two investigated cross-sections at 90° and 180°, the velocity patterns have been completely redistributed. This redistribution effect is considerable in the downstream part of the bend where the outer bank scour has been reduced and shifted towards the middle of the cross-section. The bed profile is flatter than in the reference experiment without the bubble screen and the development of the inner point bar has been avoided. However, the bubble screen was too weak to counteract the upstream straight flow impingement and, consequently, the first main scour hole was not modified.

The bubble screen technique is supposed to be more efficient in mildly and moderately curved channels where the strength of the curvature-induced secondary flow is weaker than in sharply curved channels. The reduction of scour obtained in the presented laboratory experiments is indicative as it should be strongly dependant of other characteristics such as the sediment size and distribution, the cross-section geometry, bend curvature and the width-to-depth ratio.

V ACKNOWLEDGEMENTS

This research was financially supported by the Swiss National Science Foundation under grants 200021-125095. The second author was partially funded by the Chinese Academy of Sciences fellowship for young international scientists under Grant No. 2009YA1-2 and by the Sino-Swiss science and technology cooperation for the joint research project GJH20908.

VI REFERENCES

Abad J. D., & Garcia M. H. (2009). – Experiments in a high-amplitude Kinoshita meandering channel: 2. Implications of bend orientation on bed morphodynamics. *Water Resources Research,* **45**, W02402, doi:10.1029/2008wr007017.

Blanckaert K., & Graf W. H. (2001). – Mean flow and turbulence in open-channel bend. *Journal of Hydraulic Engineering-ASCE,* **127(10)**: 835-847.

Blanckaert K., & Lemmin U. (2006). – Means of noise reduction in acoustic turbulence measurements. *Journal of Hydraulic Research,* **44(1)**: 3-17.

Blanckaert K., Buschman F. A., Schielen R., & Wijbenga J. H. A. (2008). – Redistribution of velocity and bed-shear stress in straight and curved open channels by means of a bubble screen: Laboratory experiments. *Journal of Hydraulic Engineering-ASCE,* **134(2)**:184-195.

Blanckaert K. (2010). – Topographic steering, flow recirculation, velocity redistribution, and bed topography in sharp meander bends. *Water Resources Research,* **46**, W09506, doi:10.1029/2009WR008303.

Dugué V., Blanckaert K., & Schleiss A. J. (2011). – Influencing bend morphodynamics by means of an air-bubble screen - Topography and velocity field. *Proc. of the 7th IAHR Symp. on River, Coastal and Estuarine Morphodynamics,* Beijing, China.

Ferguson R. I., Parsons D. R., Lane S. N., & Hardy R. J. (2003). – Flow in meander bends with recirculation at the inner bank. *Water Resources Research*, **39(11)**: 1322.

Frothingham K. M., & Rhoads, B. L. (2003). – Three-dimensional flow structure and channel change in an asymmetrical compound meander loop, Embarras River, Illinois. *Earth Surface Processes and Landforms,* **28(6)**: 625-644.

Hurther D., & Lemmin U. (1998). – A constant-beam-width transducer for 3D acoustic Doppler profile measurements in open-channel flows. *Measurement Science and Technology,* **9(10)**: 1706-1714.

Lemmin U., & Rolland T. (1997). – Acoustic velocity profiler for laboratory and field studies. *Journal of Hydraulic Engineering-ASCE*, **123(12)**: 1089-1098.

Nakai M., & Arita M. (2002). – An experimental study on prevention of saline wedge intrusion by an air curtain in rivers. *Journal of Hydraulic Research*, **40(3)**: 333-339.

Odgaard A. J. (1981). – Transverse bed slope in alluvial channel bends. *Journal of the Hydraulics Division-ASCE,* **107(12)**: 1677-1694.

Odgaard A. J., & Kennedy J. F. (1983). – River-bend bank protection by submerged vanes. *Journal of Hydraulic Engineering-ASCE,* **109(8)**: 1161-1173.

Roca M., Martin-Vide J. P., & Blanckaert K. (2007). – Reduction of bend scour by an outer bank footing: Footing design and bed topography. *Journal of Hydraulic Engineering-ASCE,* **133(2)**: 139-147.

Roca M., Blanckaert K., & Martin-Vide J. P. (2009). – Reduction of bend scour by an outer bank footing: Flow field and turbulence. *Journal of Hydraulic Engineering-ASCE,* **135(5)**: 361-368.

Schladow S. G. (1993). – Lake destratification by bubble-plume systems - design methodology. *Journal of Hydraulic Engineering-ASCE,* **119(3)**: 350-368.

Struiksma N., Olesen K. W., Flokstra C., & de Vriend H. J. (1985). – Bed deformation in curved alluvial channels. *Journal of Hydraulic Research,* **23(1)**: 57-79.

Whiting P. J., & Dietrich W. E. (1993). – Experimental studies of bed topography and flow patterns in large-amplitude meanders. 1. Observations. *Water Resources Research,* **29(11)**: 3605-3614.